

Article

Heterochronic origin of spherical fusulinid foraminifera in the late Paleozoic

Yukun Shi 

Abstract.—Heterochrony describes acceleration, displacement, and/or retardation of descendants' development events compared with ancestral states and has often been cited as an important process to bring about morphological novelty. It was coined one-and-a-half centuries ago and has been discussed by both paleobiologists and biologists frequently ever since. Many types of fossil organisms preserve aspects of their development histories in their bones or shells that have been used for heterochrony analyses, with body size being used as a developmental age indicator, despite questions being raised regarding this practice. For organisms whose hard structures consist of multiple chambers, or that contain growth lines, age information suggested by these structures independently can facilitate ontogenetic modeling. In this way, relations among size, shape, and age can be established to document patterns of morphological development.

Morphological analysis of pseudoschwagerine fusulinids, a fossil foraminifera group that developed a morphologically novel spherical shell, along with their presumptive triticitid ancestors illustrates this approach to heterochrony analysis. Ontogenetic trajectory comparisons of four major pseudoschwagerine genera, as well as those of triticitids, document relations between their shapes, sizes, and developmental ages. A complex of heterochronic patterns, including peramorphic predisplacement, hypermorphosis, and acceleration, characterize pseudoschwagerine development and appear to be responsible for the novel appearance of large, inflated fusiform and spherical tests in these late Paleozoic benthic foraminifera. The morphometric approach employed in this investigation could be applied widely in the quantitative morphological studies of development histories in a variety of other fossil groups.

Yukun Shi. *Centre of Science and Education for Biological Evolution and Environment, Nanjing University, Nanjing 210023, China. E-mail: ykshi@nju.edu.cn*

Accepted: 23 October 2020

Data available from the Dryad Digital Repository: <https://doi.org/10.5061/dryad.sn02v6x26>

Introduction

Among all development and phylogeny-related topics, heterochrony has been described consistently as an evolutionary process capable of bringing about macroevolutionary change. Both the term and the concept were coined by Haeckel (1866) when he proposed his “biogenetic law,” also called the theory of recapitulation. The initial definition was under the category of cenogenesis, as displacements of developmental time or dislocations of the phylogenetic order of succession, and has oftentimes been associated with the condensation of ancestral adult stages in descendants (Haeckel 1866; Gould 1977).

Heterochrony is here accepted as “change in timing or rate of developmental events, relative to the same events in the ancestor” (McKinney and McNamara 1991: p. 387). Different models

have been suggested to describe the processes it includes. Besides eight morphogenetic modes raised by De Beer (1930) and the clock model of Gould (1977), Alberch et al. (1979) placed heterochrony within a strictly quantitative formalism and introduced an ontogenetic trajectory through a multidimensional space to record shape and size development along with age. Through the 1980s to the present, heterochrony studies have expanded to include all temporal-related morphological changes, including whole body, organs, and morphological traits (McNamara 1986; McKinney and McNamara 1991; O’Keefe et al. 1999; Cartolano et al. 2015; Foth et al. 2016; Dial et al. 2017; Godoy et al. 2018), and heterochronic processes have been often simplified and presented in a two-dimensional (2D) shape–size plane.

© The Author(s), 2020. Published by Cambridge University Press on behalf of The Paleontological Society. This is an Open Access article, distributed under the terms of the Creative Commons Attribution-NonCommercial-ShareAlike licence (<http://creativecommons.org/licenses/by-nc-sa/4.0/>), which permits non-commercial re-use, distribution, and reproduction in any medium, provided the same Creative Commons licence is included and the original work is properly cited. The written permission of Cambridge University Press must be obtained for commercial re-use.

0094-8272/21

Time and phylogeny have been two basic components of heterochrony concepts since their original formulation (Haeckel 1866, 1905; Cope 1896; Gould 1977; Fink 1982; Klingenberg 1998). But for fossils, developmental times are often difficult to measure. Thus, body size has frequently been used as a developmental age proxy (e.g., Wei 1994; Zollikofer and Leon 2006; Foth et al. 2016; Dial et al. 2017), despite its inaccuracy as an age indicator (Buddemeier et al. 1974; Shea 1983; Emerson 1986; Jones 1988; Oschmann 2009). If growth curves are plotted in a 2D shape–size space, distinctions between size and age are necessarily confounded, and misinterpretations can result, as significantly different trajectories in shape–size–age space could appear similar (McKinney 1988).

The analysis of heterochronic patterns in a 2D size–shape space is also incompatible with the concept of complex heterochrony. Different from the single heterochronic process that resulted in morphological change, complex heterochrony refers to the combination of heterochronic processes affecting the same parameter, that is, shape or trait (Neige et al. 1997), and has long been referred to as a common observation (Alberch et al. 1979; Dommergues et al. 1986; Klingenberg 1998). Combinations of two (or more) heterochronic processes have been found to characterize a number of evolutionary changes (Dommergues et al. 1986; Klingenberg and Spence 1993; Neige et al. 1997; Klingenberg 1998; Godoy et al. 2018). Unfortunately, when two or more processes are present, the geometry of their effect(s) can be difficult to resolve in this simple space, because size–shape correlated growth patterns may display little apparent conformance to any single process (Godoy et al. 2018) or may exhibit the mimetic process in others (Neige et al. 1997). Regardless, size and shape are two independent morphological indicators and might suggest the operation of different relative growth processes if they are studied separately in the context of an appropriate age indicator.

In the case of organisms whose shells or bones preserve the aspects of size, shape, and developmental stage, combined heterochronic processes can be explored in their shape–size–age relations thoroughly. The growth rings of mollusks and cephalopods, chamber septa

number of ammonites, and chamber and whorl numbers of foraminifera all have been used to estimate organism ages (Doguzhaeva 1982; Dommergues 1988; Bucher and Guex 1990; Neige et al. 1997; Shi and MacLeod 2016). Indeed, the chambers or whorls of many fossil taxa contain many valid developmental time indicators such that their shape and size ontogenies can be studied separately to investigate complex patterns of heterochrony.

Fusulinids, the oldest larger benthic foraminifera, lived in shallow-marine late Paleozoic environments (Ross 1995; Hohenegger 2011) and built multichambered shells, often called tests, with planispirally coiled chambers. Test growth in foraminifera is believed to reflect the growth of the internal cytoplasmic mass (Hohenegger and Briguglio 2014), and these chambered tests record the size and shape development at discrete states of ontogeny. The developmental histories of fusulinid tests can be revealed in thin section. Axial thin sections (Fig. 1A,B), produced by grinding the test parallel to the coiling axis until the center of the initial chamber or proloculus is exposed, present the interior test morphology as well as the test's cross-sectional form of each whorl. As a result, the forms of all fusulinid tests can be observed, measured, and studied quantitatively at each whorl-based stage of their ontogenetic development.

In the evolutionary history of fusulinids, there is one significant taxonomic radiation event in the early Permian associated with the macroevolutionary occurrence of a new group with large inflated tests, namely *Pseudoschwagerininae* Zhang, 1963 (Leven 1993; Shi and Yang 2005; Yang et al. 2005), and there has long been a suspicion among fusulinid taxonomists that a heterochronic process might have been responsible for this morphological novelty. *Pseudoschwagerina* and an earlier-evolved genus belonging to the same Schwagerinidae family, namely *Triticites*, both developed similar fusiform juvenile tests with identical keriotheca-containing test walls and distinct chomata (black parallel ridge pairs deposited to prevent cytoplasmic scattering); therefore, the latter is considered the presumptive pseudoschwagerine ancestor (e.g., Ross 1967; Rozovskaya 1975; Sheng et al. 1988;

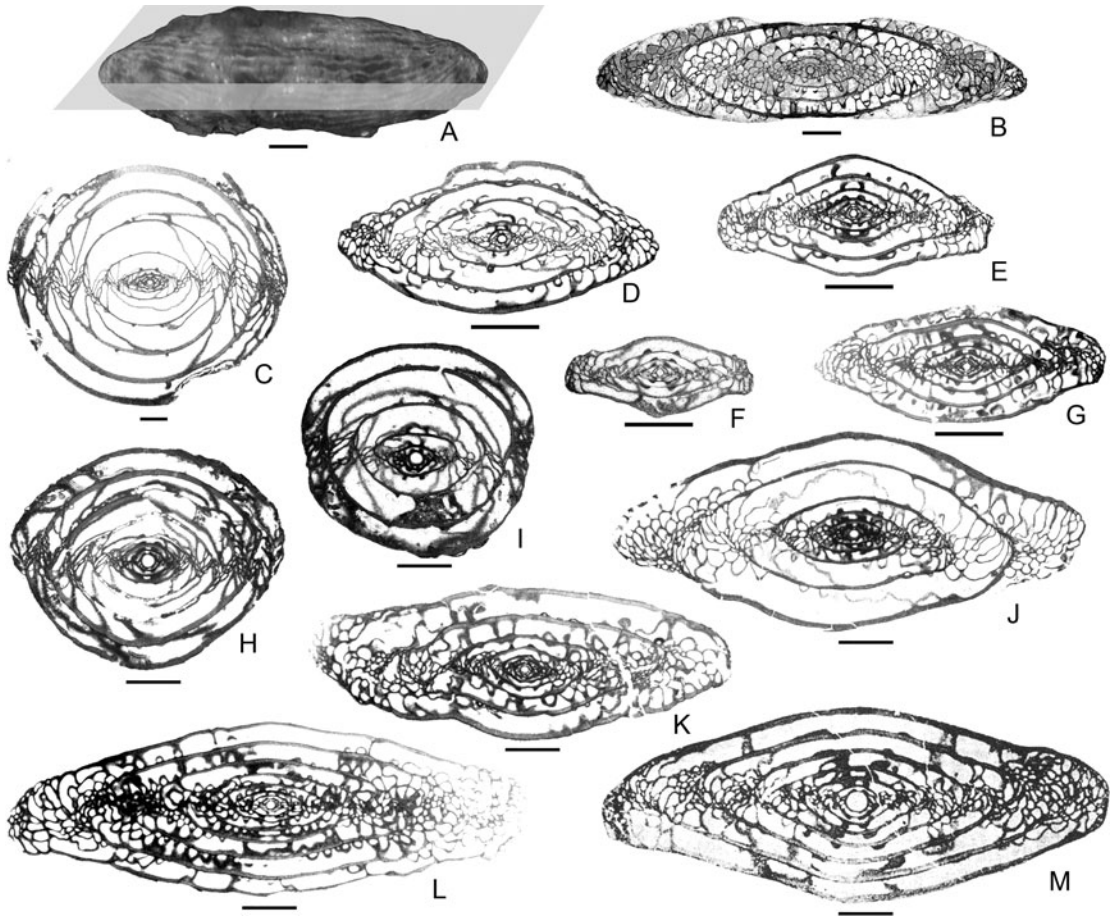


FIGURE 1. The whorl exterior test and axial thin sections of fusulinids. A, Fusulinid individual sample displaying a grind direction of axial section; B, an axial section of sample A; C–M, species used in the analysis: C, *Sphaeroschwagerina constans*; D, *Pseudoschwagerina neotruncata*; E, *Triticites creekensis*; F, *Triticites concaviclivis*; G, *Triticites noinskyi*; H, *Zellia colaniae*; I, *Robustoschwagerina yishanensis*; J, *Pseudoschwagerina subconvexa*; K, *Triticites stuckenbergi*; L, *Triticites* cf. *T. vicrotioensis*; M, *Triticites cellamagnus*. Scale bars, 1 mm.

Yang and Hao 1991; Yang 1992; Leven 1993). While all triticitid species retain a fusiform test shape in their adult life-history stage, pseudoschwagerine species adopted a loosely coiled and hugely inflated fusiform, subspherical or spherical test in the adult stage. The significant shape and size differences exhibited by triticitid and pseudoschwagerine species document a substantial level of morphological divergence in the pseudoschwagerine lineage.

Of the several pseudoschwagerine genera, *Robustoschwagerina* has been regarded as having evolved through hypermorphosis (Yang and Hao 1991; Yang 1992). While the morphological analyses in these studies were incomplete, they raise the questions of whether

the pseudoschwagerine lineage resulted from heterochronic modification of ancestral developmental conditions and which heterochronic pattern, or combination of patterns, was responsible for this macroevolutionary event. The present study aims to test several related hypotheses, including: (1) whether geometric morphometric routine could be employed to expose heterochronic pattern during developmental history of fusulinid foraminifera; (2) whether a single or complex heterochronic pattern reflects the mechanism responsible for the pseudoschwagerine evolution in the early Permian; and (3) whether the commonly used shape and size correlation would bias a heterochronic analysis.

Materials

The Pseudoschwagerininae appeared abruptly in the early Permian fusulinid radiation. Among the four genera mainly developed in this radiation, *Pseudoschwagerina*, *Robustoschwagerina*, *Sphaeroschwagerina*, and *Zellia*, *Pseudoschwagerina* exhibits inflated fusiform to subspherical adult test forms (Fig. 1D,J), while the other three exhibit subspherical to spherical test forms (Fig. 1C,H,I). Another schwagerinid genus, *Triticites*, has long been considered the likely genus into which the pseudoschwagerine ancestor would be placed (e.g., Ross 1967; Rozovskaya 1975; Yang and Hao 1991; Yang 1992; Leven 1993).

The present study included 66 specimens belonging to pseudoschwagerine genera (15 *Pseudoschwagerina*, 24 *Robustoschwagerina*, 14 *Sphaeroschwagerina*, and 13 *Zellia*; see Table 1). Forty *Triticites* specimens, including 21 from the late Carboniferous as the ancestor group and 19 from the early Permian as descendants, were also recruited. Among all the specimens, 100 were collected or reported from China and 6 were from other countries (Table 1). The Carboniferous triticitid forms are morphologically close and therefore most likely have a phylogenetic connection to the pseudoschwagerine species of this study. Examples include *Triticites concaviclivis* (Fig. 1F) as the possible ancestor of *Sphaeroschwagerina constans* (Fig. 1C), both having tightly coiled juvenile whorls with medium-sized proloculi, slim spirotheca, and small but distinct chomata; *Triticites creekensis* (Fig. 1E) as the possible ancestor of *Pseudoschwagerina neotruncata* (Fig. 1D) for their loosely coiled juvenile whorls, medium-sized proloculi, and narrow and distinct chomata; and *Triticites noinskyi* (Fig. 1G) as the possible ancestor of the pseudoschwagerine species exhibiting loosely coiled juvenile whorls, large proloculi, and strong and wide chomata, such as *Robustoschwagerina yishanensis* (Fig. 1I), *Zellia colaniae* (Fig. 1H), and *Pseudoschwagerina subconvexa* (Fig. 1J).

The Permian triticitid species were selected for analysis to represent the developmental history of descendants with fusiform tests. Most Permian triticitid species are distinct from Carboniferous species for developing strongly

folded septa and large fusiform tests with more whorls, but the identical inner whorls between species disclose the phylogenetic relationships. Examples include Permian *Triticites stuckenbergi* (Fig. 1K) as the possible descendant of Carboniferous *Triticites* cf. *T. vicrotioensis* (Fig. 1L) as both developed small proloculus, slim but distinct chomata, and slightly folded septa in the inner whorls; and *T. noinskyi* as the possible ancestor of Permian *Triticites cellamagnus* (Fig. 1M) as both developed large proloculi, distinct chomata, and straight septa in the inner whorls.

It is uncertain at present which species are the direct ancestors of the studied pseudoschwagerine and Permian triticitid species, and the morphologies of these taxa might well vary in some small respects from the presumed ancestor forms. Chances would be rare for some South China triticitids as ancestors of the American Permian triticitids. The strategy of mixing multiple species of each genus was therefore conducted to combine patterns of morphological variation into averaged morphologies, to achieve unbiased representation of the ancestor and descendant groups. Altogether, six groups—Carboniferous *Triticites*, Permian *Triticites*, *Pseudoschwagerina*, *Robustoschwagerina*, *Sphaeroschwagerina*, and *Zellia*, were the main focus of comparison and discussion through the entire analysis.

Methods

Thin sections of South China specimens (99 in total) were photographed, and seven previously published specimen images were rescanned to obtain high-resolution representations of the axial-sectional morphology. Ontogenetic test-form growth patterns were quantified using the tpsDig program via representations of changes in the axial-sectional outline of successive growth stages (see Shi and MacLeod 2016). To facilitate comparison, the growth interval was set to coincide with chamber whorl formation, irrespective of the actual time interval between successive chamber secretions. The final chamber of each half whorl was exposed in the axial section and therefore numbered to represent the growth interval as a whorl stage. Each axial section

TABLE 1. Species in the analysis

Species	Specimen no.	Collecting sites	References
Asselian-Sakmarian (Permian) <i>Robustoschwagerina</i>	24		
<i>R. xiaodushanica</i> Sheng, Wang, and Zhong, 1984	8	Zongdi Section, Guizhou, South China	Two from Shi et al. 2012: plate XX, figs. 11, 16; six unpublished data
	1	Bianping Section, Guizhou, South China	Xiao et al. 1986: plate 6, fig. 6
<i>R. guangxiensis</i> (Yang in Yang and Hao, 1991)	1	Zongdi Section, Guizhou, South China	Unpublished data
	3	Yishan Section, Guangxi, South China	Unpublished data
<i>R. yishanensis</i> (Yang in Yang and Hao, 1991)	5	Zongdi Section, Guizhou, South China	Four from Shi et al. 2012: plate XX, figs. 1, 4, 5, 13; one unpublished
	1	Yishan Section, Guangxi, South China	Yang and Hao 1991: plate II, fig. 7
<i>R. regularis</i> (Yang in Yang and Hao, 1991)	1	Xiaodushan Section, Guangxi, South China	Sheng et al. 1984: plate 1, fig. 8
<i>R. schellwieni</i> (Yabe in Hanzawa, 1939)	2	Kalpin, Xinjiang, North China	Zhang 1963: plate VIII, fig. 4; plate IX, fig. 11
<i>R. tumida</i> (Likharev, 1934)	1	Darwas, Tajikistan	Likharev 1939: plate 4, fig. 1
<i>R. sp.</i>	1	Guangxi	Unpublished data
Asselian-Sakmarian (Permian) <i>Sphaeroschwagerina</i>	14		
<i>S. constans</i> (Shcherbovich in Rauser-Chernousova and Shcherbovich, 1949)	5	Zongdi Section, Guizhou, South China	One from Shi et al. 2012: plate 21, fig. 1; four unpublished data
<i>S. karnica</i> (Schellwien, 1898)	1	Yishan Section, Guangxi, South China	Unpublished data
<i>S. glomerosa</i> (Schwager, 1883)	2	Kalpin, Xinjiang, North China	Zhang 1963: plate VII, figs. 1, 3
<i>S. sphaerica gigas</i> (Shcherbovich in Rauser-Chernousova and Shcherbovich, 1949)	1	Yishan Section, Guangxi, South China	Chen and Wang 1983: plate 24, fig. 3
<i>S. subrotunda</i> (Ciry, 1943)	1	Kalpin, Xinjiang, North China	Zhang 1963: plate VIII, fig. 1
	2	Zongdi Section, Guizhou, South China	Unpublished data
	2	Southern Guizhou, South China	Zhang et al. 2010: plate 42, figs. 4, 10
Asselian-Sakmarian (Permian) <i>Pseudoschwagerina</i>	15		
<i>P. aequalis</i> Kahler and Kahler, 1937	1	Zongdi Section, Guizhou, South China	Shi et al. 2012: plate XIX, fig. 1
<i>P. broggii</i> Roberts, 1949	1		Shi et al. 2012: plate XVIII, fig. 3
<i>P. convexa</i> Thompson, 1954	1		Shi et al. 2012: plate XVIII, fig. 16
<i>P. miharanoensis</i> Akagi, 1958	1		Shi et al. 2012: plate XIX, fig. 12
<i>P. neotruncata</i> (Shi in Shi et al., 2009a)	2		Shi et al. 2009a: plate III, figs. 1, 2, 5
<i>P. nitida</i> Kahler and Kahler, 1937	1		Shi et al. 2012: plate XVIII, fig. 10
<i>P. subconvexa</i> (Shi in Shi et al., 2009a)	1		Shi et al. 2009a: plate III, fig. 11
<i>P. texana</i> Dunbar and Skinner, 1937	1		Shi et al. 2012: plate XVIII, fig. 12
<i>P. zhongzanica</i> Zhang, 1982	2		Shi et al. 2012: plate XIX, figs. 4, 7
<i>P. tinvenkiangi</i> (Lee, 1927)	1	Riwoqe, Tibet, South China	Zhang 1982: plate 9, fig. 7
<i>P. beedei</i> Dunbar and Skinner, 1937	1	Southern Guizhou, South China	Zhang et al. 2010: plate 39, fig. 11
<i>P. ishimbajica fulx</i> (Rauser-Chernousova in Rauser-Chernousova and Shcherbovich, 1949)	1		Zhang et al. 2010: plate 38, fig. 11
<i>P. truncata</i> (Rauser-Chernousova in Rauser-Chernousova and Shcherbovich, 1949)	1		Zhang et al. 2010: plate 38, fig. 8
Asselian-Sakmarian (Permian) <i>Zellia</i>	13		
<i>Z. colaniae</i> (Kahler and Kahler, 1937)	2	Zongdi Section, Guizhou, South China	Shi et al. 2012: plate XXII, figs. 5, 7

Table 1. Continued.

Species	Specimen no.	Collecting sites	References
<i>Z. magna-sphaerae</i> Colani, 1924	2		Shi et al. 2012: plate XXII, figs. 6, 13
<i>Z. ziyunica</i> Zhang et al., 1988	1		Shi et al. 2012: plate XXII, fig. 3
<i>Z. crassialveola</i> Zhang, 1963	4	Kalpin, Xinjiang, North China Southern Guizhou, South China	Zhang 1963: plate IX, fig. 12 Zhang et al. 2010: plate 40, figs. 5, 6, 8 Zhang et al. 2010: plate 40, figs. 3, 4 Zhang et al. 2010: plate 40, fig. 23 Zhang et al. 2010: plate 41, fig. 10
<i>Z. chengkungensis</i> Sheng, 1949	2		
<i>Z. elliptica</i> Zhou and Yang, 1996	1		
<i>Z. galatea</i> (Ciry, 1943)	1		
Gzhelian (Carboniferous) <i>Triticites</i>	21		
<i>T. bashkiricus</i> Rozovskaya, 1950	1	Southeastern Yunnan, South China	Chen et al. 1991: plate VIII, fig. 15
<i>T. concaviclivis</i> Yang, 1982	1	Zongdi Section, Guizhou, South China	Shi et al. 2012: plate V, fig. 12
<i>T. communis krosnoglinskensis</i> Rauser-Chernousova, 1958	1		Shi et al. 2012: plate VI, fig. 18
<i>T. insolentis</i> Chen et al., 1991	1	Southeastern Yunnan, South China	Chen et al. 1991: plate V, fig. 24
<i>T. noinskyi</i> Rauser-Chernousova, 1938	1	Zongdi Section, Guizhou, South China	Shi et al. 2012: plate IV, fig. 7
<i>T. ovalis</i> Rozovskaya, 1950	1		Shi et al. 2012: plate V, fig. 10
<i>T. pseudoarcticus</i> Rauser-Chernousova, 1938	1		Shi et al. 2012: plate IV, fig. 23
<i>T. petschoricus</i> Rauser-Chernousova and Belyaev in Rauser-Chernousova et al., 1936	1	Pechora, North Russia	Rauser-Chernousova et al. 1936: plate 2, fig. 14
<i>T. pajerensis</i> Roberts, 1949	1	Zongdi Section, Guizhou, South China	Shi et al. 2012: plate VI, fig. 20
<i>T. primarius</i> Merchant and Keroher, 1939	1	Southeastern Yunnan, South China	Chen et al. 1991: plate VIII, fig. 23
<i>T. primitivus</i> Rozovskaya, 1950	1		Chen et al. 1991: plate VII, fig. 4
<i>T. pseudopusillus</i> Liu, Xiao and Dong, 1978	1	Southern Guizhou, South China	Zhang et al. 1988: plate 3, fig. 7
<i>T. stuckenbergi</i> Rauser-Chernousova, 1938	1	Zongdi Section, Guizhou, South China	Shi et al. 2012: plate IV, fig. 34
<i>T. schwageriniformis</i> Rauser-Chernousova, 1938	1	Southern Guizhou, South China	Zhang et al. 1988: plate I, fig. 19
<i>T. shikhanensis</i> Rozovskaya, 1950	1	Southern Guizhou, South China	Zhang et al. 1988: plate I, fig. 32
<i>T. sinuosus</i> Rozovskaya, 1950	2	Zongdi Section, Guizhou, South China	Shi et al. 2012: plate IV, figs. 30, 33
<i>T. simplex</i> (Schellwien, 1908)	1	Southern Guizhou, South China	
<i>T. springvillensis</i> Thompson, Verville and Bissell, 1950	1	Zongdi Section, Guizhou, South China	Shi et al. 2012: plate V, fig. 4
<i>T. subventricosus</i> Dunbar and Skinner, 1937	1		Shi et al. 2012: plate V, fig. 35
<i>T. variabilis</i> Rozovskaya, 1950	1		Shi et al. 2012: plate IV, fig. 11
Asselian-Sakmarian (Permian) <i>Triticites</i>	19		
<i>T. bensonensis</i> Ross and Tyrrell, 1965	1	Southeastern Yunnan, South China	Chen and Wang 1983: plate XI, fig. 16
<i>T. cellamagnus</i> (Thompson and Beissel in Thompson, 1954)	1	Utah, USA	Thompson 1954: plate 11, fig. 1
<i>T. confertus</i> Thompson, 1954	1	Texas, USA	Thompson 1954: plate 8, fig. 14
<i>T. kueichihensis</i> Chen, 1934	1	Zongdi Section, Guizhou, South China	Shi et al. 2012: plate VI, fig. 16
<i>T. longus formosus</i> Rozovskaya, 1950	1		Shi et al. 2012: plate VII, fig. 20
<i>T. minutus</i> (Lee, 1927)	1	Southern Guizhou, South China	Zhang et al. 1988: plate 2, fig. 16
<i>T. neokawensis</i> (Shi in Shi et al., 2009a)	1	Zongdi Section, Guizhou, South China	Shi et al. 2009a: plate I, fig. 22
<i>T. neoyunnanica</i> Chen et al., 1991	1		Shi et al. 2012: plate V, fig. 5
<i>T. provensis</i> Thompson, Verville and Bissell, 1950	1		Shi et al. 2012: plate V, fig. 21
<i>T. pseudosimplex</i> Chen, 1934	1		Shi et al. 2012: plate VII, fig. 14
<i>T. quasivulgaris</i> (Lee, 1927)	1		Shi et al. 2012: plate VI, fig. 17

<i>T. rockensis</i> Thompson, 1954	1	Kansas, USA	Thompson 1954: plate 9, fig. 16
<i>T. secaticus</i> (Say in James, 1823)	1	Volga, Southwest Russia	Rausser-Cernoussova 1938: plate 4, fig. 2
<i>T. ventricosus inflatus</i> (Galloway and Ryniker in White, 1932)	1	Zongdi Section, Guizhou, South China	Shi et al. 2012: plate VI, fig. 19
<i>T. cf. T. victoricensis</i> Dunbar and Skinner, 1937	1		Shi et al. 2012: plate VII, fig. 19
<i>T. volgensis</i> Rausser-Chernoussova, 1938	1	Volga, Southwest Russia	Rausser-Cernoussova 1938: plate 5, fig. 7
<i>T. yunnanica</i> Chen et al., 1991	1	Southeastern Yunnan, South China	Chen et al. 1991: plate VII, fig. 8
<i>T. zhangxi</i> Chen and Wang, 1983	1	Guangxi, South China	Chen and Wang 1983: plate X, fig. 18
<i>T. ziyunensis</i> Zhang et al., 1988	1	Zongdi Section, Guizhou, South China	Shi et al. 2009a: plate I, fig. 25

image was edited to expose a series of outlines illustrating the overall form of the test at each whorl stage (Fig. 2). Test outline at each whorl stage was digitized by specification of four type 2 landmarks, located at the maxima of curvatures (Bookstein 1986), and 36 semilandmarks representing the interlandmark curve segments (Fig. 2). The number of semilandmarks required to represent these test outlines was determined by shape complexity analysis, with the outline fidelity index set to $\geq 95\%$ (MacLeod 1999; Shi and MacLeod 2016). In total, 1396 test outlines representing ontogenetic form changes in the 106 fusulinid specimens were acquired (Supplementary Material).

To study the size and shape variation aspects of fusulinid test form, generalized least-squares Procrustes superposition (Rohlf and Slice 1990) was employed to align all the outlines and normalize them for the extraneous factors of position, orientation, and size. Test size variation was quantified using the centroid size index (square root of the sum of squared distances of the landmarks in configuration to their mean location; Bookstein 1986; MacLeod 2008) and extracted from the outlines before they were aligned. Following outline alignment, principal component analysis (PCA) based on the shape covariance structure of the pooled outline dataset was used to facilitate geometric interpretation (MacLeod 2009; Shi and MacLeod 2016). When the projected scores of the outline data along the principal component axes captured various aspects of their shape variation, these scores could be used to represent the outline shapes. As a result, the specimens' ontogenetic shape trajectory could be constructed with suitable principal component scores representing the majority shape variation of the outline dataset at comparable developmental stages. Test size estimates were also added to each trajectory as a third, independent variable. The shape and size trajectories for each studied group were composed with the means of shape scores or size values of the group specimens.

Whorl stage based on half-whorl counting was regarded as the developmental age indicator in the current plots of ontogenetic variation. Chamber number is believed to be an accurate age proxy for some benthic foraminifera

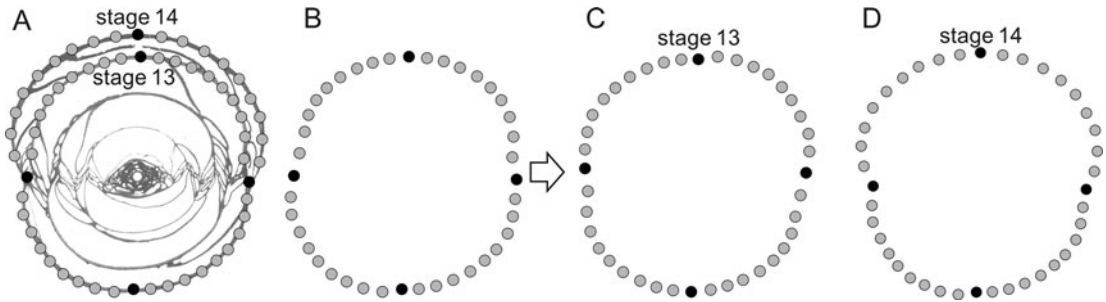


FIGURE 2. Digitization protocol for a specimen image. Outline digitized by four type 2 landmarks (black dots) and 36 other equally spaced semilandmarks (gray dots) representing the four divided segments. A, Test outlines at the successive 13th and 14th whorl stages. B,C, Outline of the odd-numbered stages (i.e., 13th) were inverted to ensure the ultimately added chamber was in an orientation consistent with those of the even-numbered stages (i.e., 14th). C,D, Standardized outlines after centroid size value has been removed.

(Hemleben et al. 1989; Speijer et al. 2008; Hohegger and Briguglio 2014), but whorl number is regarded a valid alternative for fusulinids and could be traced in the axial sections (Yang and Hao 1991; Yang 1992; Shi and MacLeod 2016). Although the true developmental time of individual whorls cannot be assumed to be equal, for the ancestor–descendant comparisons (e.g., *Pseudoschwagerininae* and *Triticites*), patterns of their whorl development and the indicated time or age interval would be similar.

Ontogenetic trajectories of the studied generic group were summarized by patterns of variation in shape (PC 1 scores), size (centroid size), and age (whorl stage), with their mean values, in a three-dimensional (3D) Cartesian space. Trajectories were projected in the 2D shape–size, shape–whorl stage, and size–whorl stage spaces to compare episodes of morphological development. Ontogenetic trajectories of all 106 specimens and six groups were plotted in the shape–whorl stage and size–whorl stage planes to isolate those aspects of the morphological development processes, including potential heterochronic pattern, involved between *triticitids* and *pseudoschwagerines*.

Results

A Fusulinid Shape Space.—A pooled shape space for the studied specimens was established through a PCA of the Procrustes-aligned outline coordinates for all specimens at each whorl stage. In total, 80 shape dimensions

account for 100% of the observed shape variance, and the first principal component summarized the overwhelming majority (75.6%) of shape structure (Fig. 3A). The first two dimensions of the PC shape space, as well as the shape models along PC 1, are shown in Figure 3.

Shape models reconstructed from the PC 1 scores identified the major shape variation among all the test outlines (Fig. 3B). Outline shapes that project to positions near the negative end along the PC 1 axis represent highly elongate fusiform shapes (e.g., close to the characteristic adult test shapes of *triticitids*), whereas those projecting to positions near the positive end demonstrate the inflated fusiform to spherical shapes similar to adult *pseudoschwagerine* tests. While juvenile tests (at 1–2 whorl stages) of most specimens have high positive PC 1 scores, the tests that developed 2–4 whorls (at 3–9 whorl stages) mostly projected in the middle area of the PC 1 axis, and mature tests of *triticitids* and *pseudoschwagerines* finally diverged to the two ends. Therefore, the PC 1 score of the outline shape can be used to quantify the primary shape change during developmental history.

Ontogenetic Trajectories and Their Projections.—Ontogenetic trajectories in the 3D shape–size–whorl stage space demonstrate the nonlinear growth pattern of the studied generic groups (Fig. 4A). Roughly two bundles of trajectories could be recognized in this space, one is composed of four *pseudoschwagerine* genera and another of the *triticitid* groups.

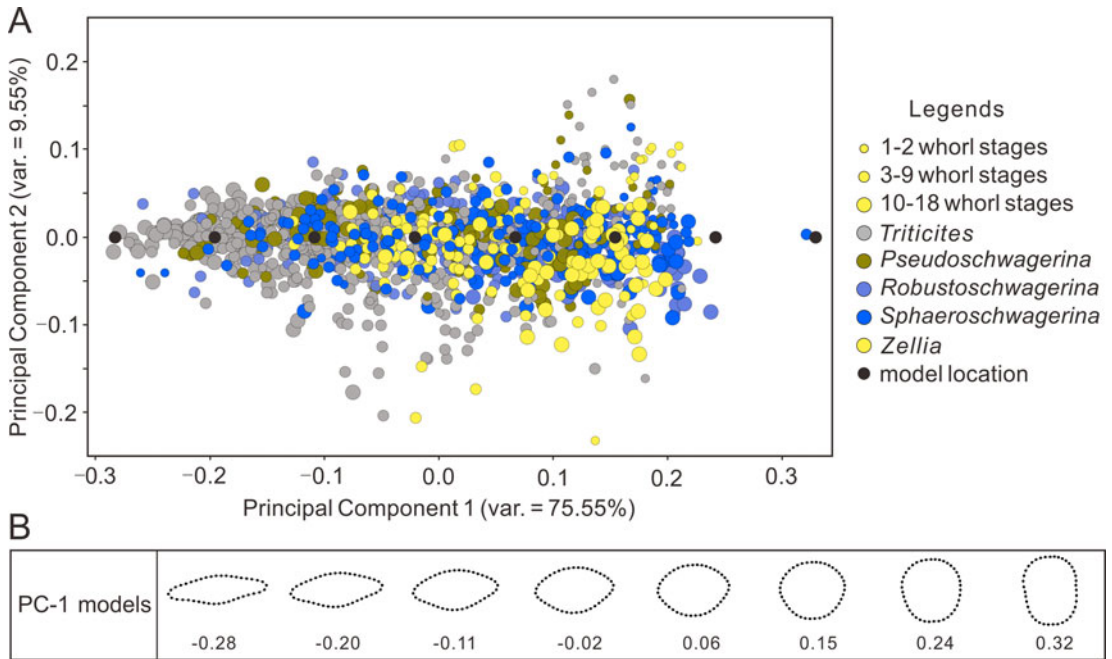


FIGURE 3. Patterns of fusulinid test shape variation represented by the first two principal components. A, Principal component analysis based on the pooled sample shape covariance matrix for all developmental whorl stages, of all specimens belonging to *Triticites* and the four genera of Pseudoschwagerinae. Test shapes of different whorl stages have been marked with circles with different radii. The positions of shape models in B are marked with black dots. B, Shape models. The models were calculated with coordinates along the PC 1 axis in the principal component shape spaces of A and are displayed with numbers representing their PC 1 coordinates.

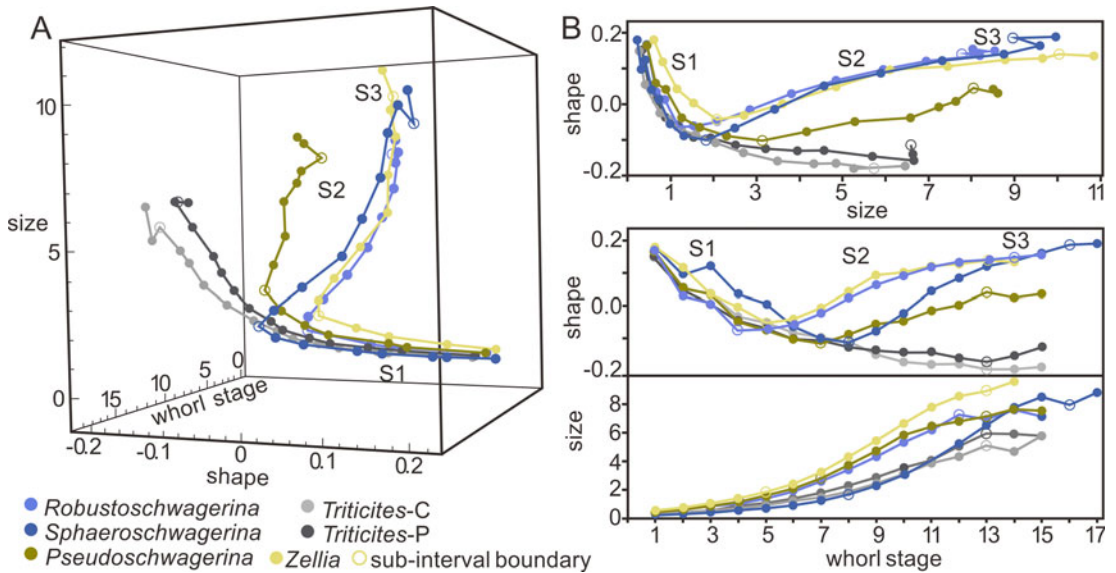


FIGURE 4. Ontogenetic trajectories of four pseudoschwagerine genera and two triticitid groups in the 3D shape–size–whorl stage space (A) and in 2D shape–size, shape–whorl stage, and size–whorl stage planes (B). Shape value is represented by PC 1 scores (no unit) and size value is represented by centroid size index (no unit). Shape and size value means of the studied species in each group are used. Error bars are not displayed to allow trajectories in 3D space and 2D planes to be distinguished.

The four pseudoschwagerine genera exhibit similar patterns, and three subintervals describing significant morphological change could be recognized in each of them. The triticitid groups present patterns formed by only two distinct subintervals, similar to the first two of the pseudoschwagerines.

The first subinterval (S1) encompasses the developmental period when all six trajectories expanded along the direction of test size, whorl stage counting increasing and shape value decreasing (Fig. 4A). It covers the first several whorl stages for pseudoschwagerines and most stages through triticitid development. S1 is followed by the second subinterval (S2), when whorl stage, test size, and shape value increased concurrently, and the curves therefore turned into a different direction. For pseudoschwagerines, S2 subintervals consist of 8 to 10 whorl stages while those of triticitids only contain two stages. The last two or three stages of pseudoschwagerines constitute the third subinterval (S3) in their development, during which whorl stage number kept increasing, test sizes slowly increased, and shape values became stable or even dropped slightly. Because of these changes, the curves' extension direction turned again and formed the distinct "tails" of the pseudoschwagerine trajectories.

These subintervals could be easily recognized in the trajectory projections in the shape-size plane (Fig. 4B). In the beginning of their development history, the six groups clustered together in the S1 subinterval, and all experienced a significant shape value drop from ca. 0.2 to ca. -0.1 within a minor size rise. After that, the divergence became evident when pseudoschwagerine shape score started to increase and their S2 subinterval started. Triticitid groups stayed in S1, and their shape value kept dropping. In S2, the sphaeroschwagerinid, robustoschwagerinid, and zellid curves clustered as their tests gradually became spherical, while test size increased significantly. The pseudoschwagerinid shape value only increased to ca. 0.05, much lower than those of the other three, describing the inflated fusiform shape of their mature tests. S3 subintervals of pseudoschwagerines are composed of the zigzag "tails" that are actually false signals resulting from variation of the mean size value.

The trajectories projections in the shape-whorl stage and size-whorl stage planes separated the shape and size variations and exhibited more regular patterns (Fig. 4C). The three subintervals could also be recognized in the shape-whorl stage but are less significant in the size-whorl stage plane. The trajectories of all species revealed more details during their developmental histories.

Ontogenetic Trajectories in the Shape-Whorl Stage Plane.—Because whorl stages were common to all fusulinids, ontogenetic trajectories can be constructed such that the test shape-phase intervals can be recognized for all the studied specimens (Fig. 5). As mentioned earlier, the ontogenetic trajectories of pseudoschwagerine species contain three recognizable form change subintervals, while triticitid species only include two and exhibit a decreasing shape value trend over most of their ontogeny.

The S1 intervals of pseudoschwagerines display a decreasing trend, with shape values dropping from 0.2 to -0.1. The proloculus is spherical in almost all foraminiferal species (Alve and Goldstein 2003; Murray 2006), and in this analysis, its shape is represented by a shape value of ca. 0.2. From this point, the developmental curves of all pseudoschwagerine species shape values decrease for four to eight whorl stages, indicating these tests altered to a fusiform shape as new chambers were added. In triticitids, S1 shape values generally continue decreasing beyond the states characteristic of pseudoschwagerines, which indicates their test shapes became more fusiform.

S2 and S3 constitute two phases of an overall inflation trend. At about the fourth (for robustoschwagerinids and zellids) or eighth (for pseudoschwagerinids and sphaeroschwagerinids) whorl stage, shape values of pseudoschwagerine tests reached their lowest, indicating the most fusiform shape the species have developed. Then pseudoschwagerines began to exhibit test inflation. During S2, their shape scores turned back toward 0.1 at about the 11th or 14th whorl stage, reflecting tests growing into spherical forms. In triticitid species, S2 does not occur until the very end of their development stages, that is, at the 12th or 13th whorl stage, where the shape score increased. This suggests that their typical fusiform shape was maintained

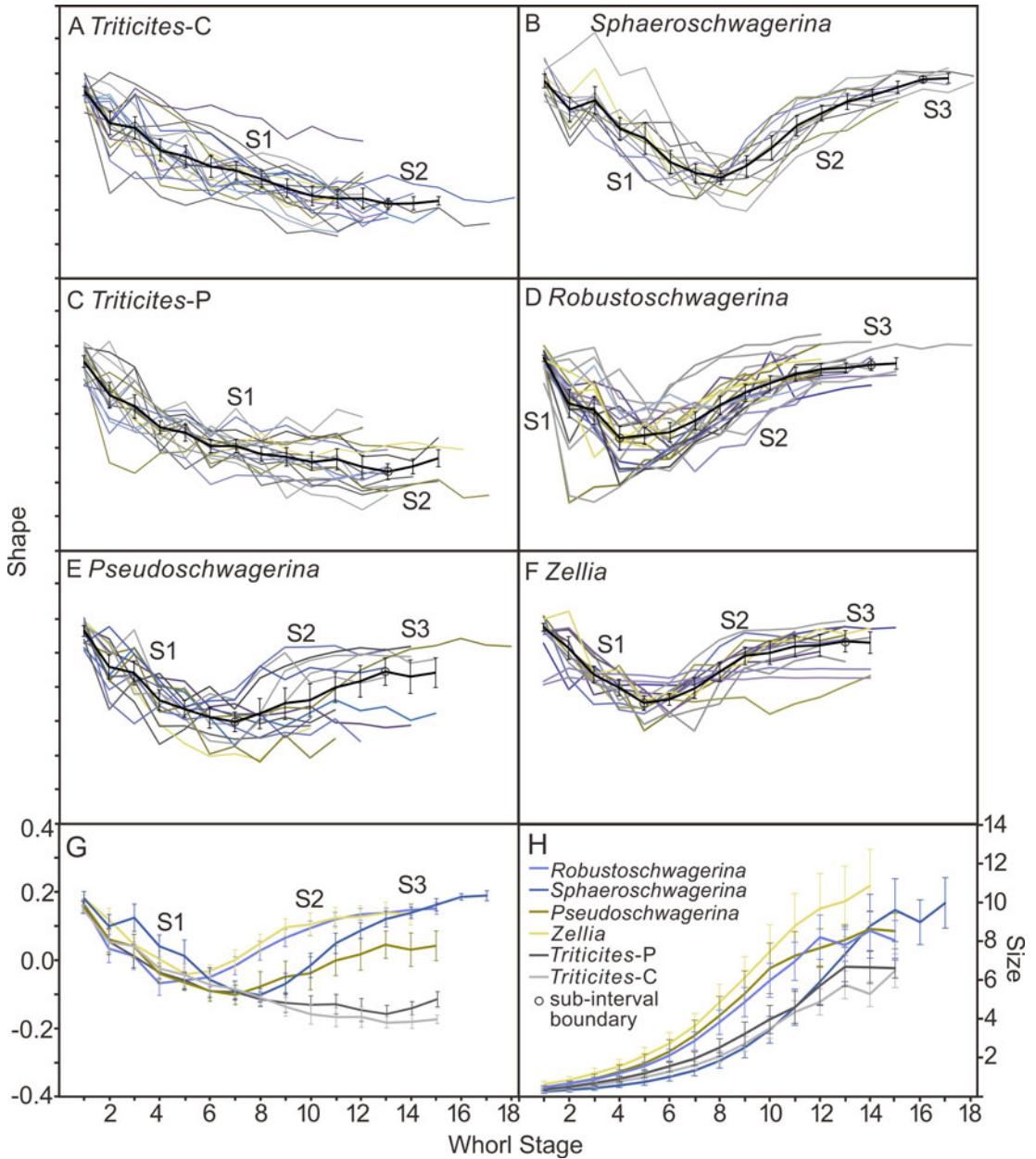


FIGURE 5. Ontogenetic shape and size trajectories of pseudoschwagerines and triticitids. A–F, Species-based shape trajectories in shape–whorl stage space. Trajectories of all studied species belonging to each genus are plotted in colored lines with pseudoschwagerine generic and triticitid group trajectories represented by mean values (black lines) of the species with 95% confidence level (black whiskers). Species list refers to Table 1. G, Assembled shape-average trajectories for four generic and two triticitid groups in the shape–whorl stage space illustrated by colored lines and whiskers. H, Size-average trajectories for pseudoschwagerine generic and two triticitid groups represented by mean values (colored lines) with 95% confidence level (colored whiskers) in size–whorl stage plane.

throughout the adult period, followed by an incipient interval of test inflation. S3 appears at the very end of the developmental sequence for all pseudoschwagerine species and is

marked by a visible turn in the developmental trajectory over the last one or two whorl stages. During this interval, the shape score of most species remained steady or exhibited a slight

drop in value, suggesting test inflation ceased when individuals entered the final (possibly the mature) stage of development.

The average shape trajectories were constructed by shape value means of the species in each group along with developmental stages. Six curves exhibit divergences in the later developmental intervals, and three assemblages can be recognized (Fig. 5G). The triticitid assemblage consists of the two triticitid groups, with a long S1 interval including about 13 whorl stages and a short S2 duration consisting of the last one or two whorl stages. The “middle” assemblage includes pseudoschwagerinid and sphaeroschwagerinid species, both with long S1 and S2 intervals that occupy nearly half of their life histories. The third assemblage consists of robustoschwagerinid and zellid species, both of which exhibit a relatively short S1 subinterval with a longer S2.

The Unique Inflation Growth of Pseudoschwagerininae Suggested by Size Change.—Size trajectories for the four pseudoschwagerine genera, as well as triticitids, all displayed exponential growth trends (Fig. 5H). Two groups are recognized based on their test size trajectories, one composed of robustoschwagerinid, pseudoschwagerinid, and zellid species (= the RPZ group) and the other composed of sphaeroschwagerinid and triticitid morphologies (= the ST group). During early ontogeny, all species increased in size slowly relative to whorl stages, and the RPZ group exhibited a markedly higher growth rate. At the fourth or fifth whorl stage, the rate of whorl-marked growth in this group increased rapidly, with zellids outpacing the other two genera. During this interval, the ST group was characterized by a notably slower whorl growth rate. As a result, the size trajectories of these groups diverged substantially.

During the 4th to 10th whorl stage, growth rates in the RPZ consistently remained several times higher than in the ST group, and test size of the zellids turned out to be the largest at their mature period. Sphaeroschwagerinid whorl growth rates are as slow as those of triticitids in their early ontogeny, until around the 10th whorl stage, but increased in apparent lockstep with test inflation after that point. In late ontogeny, that is, the 14th whorl stage,

sphaeroschwagerinid test size and shape change rates both became very similar to those of both the robustoschwagerinids and zellids, while triticitids retained a slow growth.

Discussion

In the evolution history of fusulinids, the early Permian pseudoschwagerines comprise a special branch whose taxa exhibited significant shape shifts during their ontogeny (Ross 1967; Rozovskaya 1975; Leven 1993). These spherical–fusiform–spherical test shape shifts have been quantitatively described through a geometric morphometric routine so that further comparison regarding the shift timing and process between different taxa or groups could be conducted. The advantage of the PC 1 score representing the majority of fusulinid test outline shape variation might not always be the case, but through PCA the major shape variation can be captured and investigated with sensitive procedures. Ontogenetic trajectories of fusulinid foraminifera established here provided sufficient information about their shape and size changes across their life spans and are therefore well suited to various research aims, including heterochronic analysis.

Growth curves reflecting the shape–size correspondence have been frequently used in morphological studies, including heterochronic analyses (Mitteroecker et al. 2005; Zollikofer and Leon 2006; Gerber et al. 2007; Foth et al. 2016; Dial et al. 2017). They have been established here (Fig. 4B), and the patterns are close to the ontogenetic trajectories in the 3D shape–size–whorl stage space. However, the shape–size plane failed to provide either an accurate or an adequate record of trends in size variation. In the plane, the growth curve of zellids overlapped with those of robustoschwagerinids and sphaeroschwagerinids when the size value of their tests was from two to nine, but their trajectories clearly separated in the 3D space, due to the different size growth rates (Fig. 4). To avoid this type of bias, an independent age indicator is a necessity. Creatures containing an independent, countable time record, such as chambered shells or growth lines, represent the only candidate fossil groups suitable for the detailed study of heterochrony.

The well-established theoretical relationships among size, shape, and age in the context of heterochrony analyses (Gould 1977; Alberch et al. 1979; Raff 1996), suggest that the 3D developmental space plays an important role in the analysis and comparison of heterochronic patterns, as well as in the testing of various pattern-level heterochronic hypotheses. Retention and use of all three of these critical heterochronic variables are necessary to achieve a complete understanding of any organism's developmental pathway, irrespective of taxonomic/phylogenetic level. When shape development of pseudoschwagerines, along with size increases, was quantified and compared with those of their presumptive triticitid ancestors during their life-history stages, the changes documented suggested the operation of heterochronic processes. In particular, information on developmental time in the ontogenetic trajectories could further determine whether condensation (acceleration) or retardation is displayed in pseudoschwagerine evolutionary history.

Peramorphic Heterochronic Growth of Pseudoschwagerines.—The consistent shape changes of Carboniferous triticitids and pseudoschwagerines during their early developmental stages could be observed in the current results in the form of the overlapped shape trajectories during the S1 subinterval (Fig. 5G). The divergence in their post-S1 developmental shape change can now be seen as a pseudoschwagerine apomorphy and results in the morphological distinctions between the two lineages, triticitid-represented fusiform schwagerines and inflated pseudoschwagerines.

Carboniferous triticitids developed a rather long S1 and a very short S2 (Fig. 5A). Pseudoschwagerine species repeated these two intervals, but S1 became relatively shortened and S2 extended substantially (Fig. 5B,D,F). Their shape trajectories overlapped with those of Carboniferous triticitids during the S1 interval, and S2 started at the “middle” of the Carboniferous triticitids S1, though with variation in timing. The shape trajectory of sphaeroschwagerinids diverted a bit from the others during the middle of its S1 interval but was soon back on track. S2 intervals of pseudoschwagerines developed earlier than those of their triticitid ancestors, fitting the criterion of

peramorphic predisplacement heterochrony. Their S2 intervals are much longer than the two whorl stages of Carboniferous triticitids, suggesting retardation from peramorphic hypermorphosis. Moreover, the shape changes of pseudoschwagerines during the S2 interval are faster than those of their triticitid ancestors, as indicated by the higher slopes of their S2 curves. This phenomenon indicates the peramorphic acceleration of shape change. The recapitulation of S1 and S2 ontogenetic stages of the (presumed) ancestors by descendant pseudoschwagerines, along with the developmental truncation indicated by the shortened S1, retardation indicated by the prolonged S2, and acceleration indicated by the S2 higher rate of shape change, can be attributed to the extreme shape novelties displayed by the pseudoschwagerines. In particular, the shortened S1 developmental time interval indicates peramorphic predisplacement, the developmentally prolonged S2 suggests peramorphic hypermorphosis, and higher shape change rate reveals peramorphic acceleration.

The maturity of foraminifera, both benthic and planktonic, is oftentimes indicated by the slow growth of last two whorls or chambers (Hemleben et al. 1989; Speijer et al. 2008; Hohegger 2011). In fusulinids, growth termination is coincident with the S3 subinterval. Along with the shape value plateau or drop, size growth rate of pseudoschwagerines slowed down in their end stages, that is, the 12th to 14th whorl stages (Figs. 4B, 5H). In the size-time space, the growth rates of triticitid species apparently slowed down after about the 11th whorl stage. By analogy, the decreasing or plateauing growth rate trend should be regarded as a signal of fusulinid reproductive maturity or onset of the reproduction phase of their life history. Therefore, compared with the triticitid ancestor, maturity in pseudoschwagerine genera occurred in a later stage, indicating a developmental change consistent with hypermorphosis.

Predisplacement shortened the early developmental periods of the characteristic triticitid fusiform shapes, while acceleration, expressed as an increased rate of shape change (Gould 1977; Alberch et al. 1979; Raff 1996), sped up the inflated shape change trend. Hypermorphosis is expressed by prolongation of

ontogeny, which causes delayed maturation (De Beer 1930; Gould 1977; Raff 1996). This developmental change, along with the predisplacement and acceleration, led to the expression of a radically new morphology in these triticitid descendants, such as larger body size, larger test size, and new shapes (Gould 1977; McNamara 1986).

Compared with their Carboniferous counterparts, Permian triticitids developed a similar S1 and an S2 with identical developmental time but higher shape change rate (Fig. 5A,C,H). This slight acceleration resulted in visible changes to these descendants' test shapes.

Size Rate Modification of Pseudoschwagerines.—Size change was not defined as a heterochronic process (Gould 1977; Alberch et al. 1979), but gigantism and dwarfism have long been regarded as resulting from the action of heritable changes in developmental timing (Gould 1977). Later, peramorphic acceleration was explained as increased rate of morphological development that could affect the whole organism, organs, or structures. Thus, overall size change has long been thought to be an important, though largely unacknowledged, element of heterochrony (McNamara 1986; Raff 1996; Webster and Zelditch 2005) and often represents an important factor responsible for complex morphological changes (Neige et al. 1997; McNamara and Long 2012; Godoy et al. 2018).

Ontogenetic trajectories of Carboniferous triticitid and pseudoschwagerines in the size-whorl stage space displayed exponential growth patterns (Fig. 5H). This type of size trajectory is common to most (possibly all) larger benthic foraminifera (Briguglio et al. 2011; Hohenegger and Briguglio 2014). However, the growth rates recorded by the slopes of these curves are variable. Robustoschwagerinids, sphaeroschwagerinids, and zellids exhibited higher values than their Carboniferous triticitid ancestor(s) across the whole developmental history, while sphaeroschwagerinids did not get beyond their ancestors' size growth until the 12th whorl stage. Higher size growth suggests descendants grow faster than ancestors through certain developmental stages, a pattern that can be assigned to peramorphic developmental acceleration (McNamara 1986;

Raff 1996) or recast as rate modification (Webster and Zelditch 2005). Based on these preliminary results, accelerated size growth may have existed from the beginning of development for robustoschwagerinids, pseudoschwagerinids, and zellids. However, in sphaeroschwagerinids, this trend appeared much later in the developmental sequence, although the rate increased quickly and soon exceeded that characteristic of triticitids (Fig. 5H). As a result, size acceleration appears responsible for the pronounced test-size enlargement characteristic of pseudoschwagerine fusulinids as a group.

Complex Heterochrony in Pseudoschwagerine Development.—Based on the fusulinid shape-size-whorl stage trajectories documented in this investigation, three different peramorphic heterochronies—predisplacement, hypermorphosis, and acceleration—appear to characterize pseudoschwagerine developmental history. An overall peramorphic pattern has been proposed for the development of *Robustoschwagerina* but without further detail (Yang and Hao 1991), and effects of pairwise combinations of heterochronic processes have been illustrated by Klingenberg (1998). The current morphometric routine exposed a threefold complex heterochronic pattern involving all three single peramorphic processes being responsible for the unique morphology of the four pseudoschwagerine genera. Regarding the development of a certain trait (i.e., test shape), there are altogether eight possible combinations for a threefold complex heterochronic pattern (Fig. 6), and in fact, development rate (acceleration or neoteny) and time (progenesis or hypermorphosis) are the two factors determining the trait's morphology, while the timing (predisplacement or postdisplacement) decides its relationship with other traits. In the current example, hypermorphosis indicated by the prolonged test-inflation interval (S2) and acceleration indicated by the high growth rate of both test inflation and size can explain the large, loosely coiled spherical tests of pseudoschwagerines. Predisplacement, indicated by an early start of S2, resulted in the early termination of fusiform shape development. In the commonly used shape-size space, because another important aspect of organism developmental history, size growth,

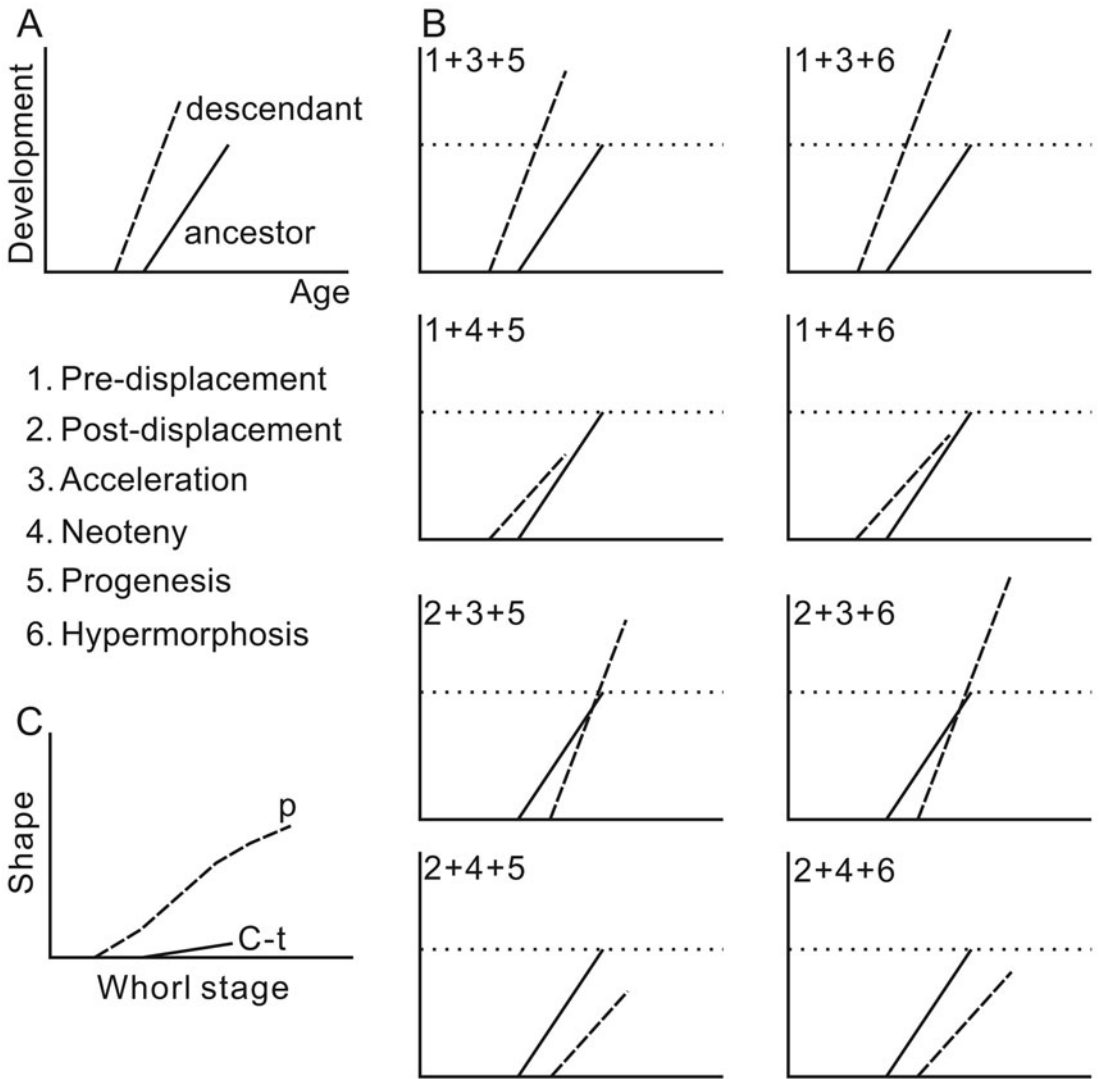


FIGURE 6. Ontogenetic trajectories effected by the threefold complex heterochronic processes and the S2 shape trajectories in the current investigation. A, Example of ancestor and descendant ontogenetic trajectories. B, Effects of the eight modes of threefold complex heterochronic processes. The simple heterochronic process involved is represented by the number. C, Simplified S2 subinterval shape trajectories of Carboniferous triticitids (C-t) and pseudoschwagerines (p).

is totally neglected, the size-related heterochronic process would be either buried or difficult to recognize. Complex heterochrony might have been overlooked in the previous research on the development history of other fossil organisms, if body size was regarded as an age indicator.

Pseudoschwagerine Thrived as K-Strategists.—The early Permian Asselian to Sakmarian stages bore witness to the fusulinid radiation in which the Pseudoschwagerinae first

appeared (Leven 1993; Shi and Yang 2005; Yang et al. 2005). Although the fusiform schwagerines remained major components of fusulinid shape diversity throughout this interval, pseudoschwagerines thrived and accounted for 14.2% of all fusulinid species occurring throughout this interval in well-studied South China stratigraphic successions (Shi et al. 2009b). As the schwagerines that flourished in this interval remained morphologically close to those of late Carboniferous species with

fusiform adult tests (e.g., *Triticites*), pseudoschwagerines constituted a considerable morphological departure from this standard. The successful radiation of pseudoschwagerines in the early Permian might be related to this radical morphological change.

Gould (1977) connected heterochronic variations in life-history strategies with r- and K-selection. Pseudoschwagerines have been regarded as representing fusulinid K-strategists (Leven 1993; Shi and Yang 2005; Yang et al. 2005), a designation they share with numerous other coeval species. The Asselian to Sakmarian interval is believed to have been a favorable time for fusulinids, with its high dissolved oxygen levels and the widespread occurrence of suitable, shallow-marine habitats (Berner 2006; Groves and Wang 2009; Payne et al. 2012). In such a stable and crowded environment, heterochronic hypermorphosis likely resulted in the retarded maturation typical of K-strategists (Gould 1977), within the pseudoschwagerine lineage, resulting ultimately in the appearance of forms characterized by large, spherical tests. The spherical test could also facilitate transportation to and colonization of new sites via selective transportation by turbulent bottom currents (Shi and MacLeod 2016).

Fusulinids are considered to have been symbiont-bearing foraminifera because of their similarities in size and internal structure to modern symbiont-bearing benthic foraminifera (Ross 1995; Groves et al. 2012). For modern symbiont-bearing foraminifera, flat and fusiform tests are usually interpreted as strategies to enlarge their test surface so more symbionts could be held within the test and exposed to sunlight (Hohenegger 2011). The spherical tests that pseudoschwagerine fusulinids developed could enhance their ability to become widely distributed, and the objective of benefiting symbionts was accomplished through large tests with large surface areas. These are probably some of the reasons for their rapid diversification, irrespective of the fact that large size would also pose biomechanical and metabolic challenges. Regardless, this diversification constituted a significant episode in the increase of diversity in the entire late Paleozoic marine invertebrate community (Fan et al. 2020).

Conclusions

Inspection of ontogenetic trajectories of organisms in the 3D shape–size–age (time) space is required to adequately represent, assess, and analyze the morphological signatures of heterochronic processes. Organisms with shells or bones that record information pertaining to specimen age are ideal subjects for such investigation. If a complete representation of this space is combined with a morphometric approach to shape characterization, morphological analyses can be used to describe the developmental histories of organisms quantitatively and so facilitate the comparisons between taxa.

With whorl stage as an independent age indicator for fusulinids, heterochronic patterns were confirmed in the development of early Permian pseudoschwagerines. Keeping in mind that both size and shape change are necessary elements for documenting complete morphological development history, ontogenetic trajectories of pseudoschwagerine fusulinids suggest that complex patterns of heterochrony were part of and served as the mechanistic basis for these morphological transitions. Peramorphic predisplacement, hypermorphosis, and acceleration of morphological development dominated the developmental history of these groups and resulted in the novel appearance of large, inflated fusiform and spherical tests in larger benthic foraminifera. Compared with their presumptive triticitid ancestor(s), pseudoschwagerine species compressed the developmental time interval in which their test morphology was characterized by a fusiform shape and added a much longer terminal stage in which the test quickly expanded to adopt a characteristic inflated or spherical shape. Accelerated test size growth was also among the trends responsible for the appearance of large pseudoschwagerine tests.

The morphometric approach presented here can successfully summarize morphological variations among organisms such as foraminifera, thus providing a common routine for various developmental investigations. The 3D shape, size, and age (time) relationship established through this procedure can quantitatively illustrate the differences and similarities

among the developmental histories of organisms and facilitate further morphological studies.

Acknowledgments

This work is supported by the National Scientific Foundation of China (grant nos. 41772017 and 91955201) and the National Key R&D Program of China (no. 2018YFE0204201). Valuable suggestions from N. MacLeod of Nanjing University, Associate Editor M. Hopkins and two anonymous reviewers are greatly appreciated. Morphometric analysis programs from Norman MacLeod have been used in the current study.

Literature Cited

- Alberch, P., S. J. Gould, G. F. Oster, and D. B. Wake. 1979. Size and shape in ontogeny and phylogeny. *Paleobiology* 5:296–317.
- Alve, E., and S. T. Goldstein. 2003. Propagule transport as a key method of dispersal in benthic foraminifera (Protista). *Limnology and Oceanography* 48:2163–2170.
- Berner, R. A. 2006. GEOCARBSULF: a combined model for Phanerozoic atmospheric O₂ and CO₂. *Geochimica et Cosmochimica Acta* 70:5653–5664.
- Bookstein, F. L. 1986. Size and shape spaces for landmark data in two dimensions. *Statistical Science* 1:181–222.
- Briguglio, A., B. Metscher, and J. Hohenegger. 2011. Growth rate biometric quantification by X-ray microtomography on larger benthic foraminifera: three-dimensional measurements push nummulitids into the fourth dimension. *Turkish Journal of Earth Sciences* 20:683–699.
- Bucher, H., and J. Guex. 1990. Rythmes de croissance chez les ammonites triasiques. *Bulletin de la Société vaudoise des sciences naturelles* 80:191–209. [In French with English abstract.]
- Buddemeier, R. W., J. E. Maragos, and D. W. Knutson. 1974. Radiographic studies of reef coral exoskeletons: rates and patterns of coral growth. *Journal of Experimental Marine Biology and Ecology* 14:179–199.
- Cartolano, M., B. Pieper, J. Lempe, A. Tattersall, P. Huijser, A. Tresch, P. R. Darrah, A. Hay, and M. Tsiantis. 2015. Heterochrony underpins natural variation in *Cardamine hirsuta* leaf form. *Proceedings of the National Academy of Sciences USA* 112:10539–10544.
- Chen, G. B., L. X. Zhang, C. F. Yang, and X. D. Wang. 1991. On the boundary between Carboniferous and Permian and the fusulinids of the boundary stratigraphy in Yunnan. *Yunnan Science and Technology Publishing House, Kunming*. [In Chinese with English abstract.]
- Chen, S. 1934. Fusulinidae of South China. *Palaeontologia Sinica series B* 4:1–185.
- Chen, X., and J. H. Wang. 1983. The fusulinids of the Maping limestone of the Upper Carboniferous from Yishan, Guangxi. *Science Press, Beijing*. [In Chinese with English abstract.]
- Ciry, R. 1943. Les Fusulinidés de Turquie—II. Le genre *Pseudoschwagerina*. *Annales de Paléontologie* 30:17–43.
- Colani, M. 1924. Nouvelle contribution à l'étude des fusulinidés de l'Extrême-Orient. *Mémoires du Service géologique de l'Indochine* 111:9–199.
- Cope, E. D. 1896. The primary factors of organic evolution. *Open Court Publishing, Chicago*.
- De Beer, G. R. 1930. *Embryology and evolution*. Clarendon, Oxford.
- Dial, T. R., D. N. Reznick, and E. L. Brainerd. 2017. Heterochrony in the evolution of Trinidadian guppy offspring size: maturation along a uniform ontogenetic trajectory. *Proceedings of the Royal Society of London B* 284:1864.
- Doguzhaeva, L. 1982. Rhythms of ammonoid shell secretion. *Lethaia* 15:385–394.
- Dommergues, J.-L. 1988. Can ribs and septa provide an alternative standard for age in ammonite ontogenetic studies? *Lethaia* 21:243–256.
- Dommergues, J.-L., B. David, and D. Marchand. 1986. Les relations ontogénèse-phylogénèse: applications paléontologiques. *Geobios* 19:335–356. [In French with English abstract.]
- Dunbar, C. O., and J. W. Skinner. 1937. Permian Fusulinidae of Texas. Pp. 517–825 in *The geology of Texas*. Vol. 3, Upper paleozoic ammonites and fusulinids. Bureau of Economic Geology Bulletin 3701. University of Texas Press, Austin.
- Emerson, S. B. 1986. Heterochrony and frogs—the relationship of a life-history trait to morphological form. *American Naturalist* 127:167–183.
- Fan, J. X., S. Z. Shen, D. H. Erwin, P. M. Sadler, N. MacLeod, Q. M. Cheng, X. D. Hou, J. Yang, X. D. Wang, Y. Wang, H. Zhang, X. Chen, G. X. Li, Y. C. Zhang, Y. K. Shi, D. X. Yuan, Q. Chen, L. N. Zhang, C. Li, and Y. Y. Zhao. 2020. A high-resolution summary of Cambrian to Early Triassic marine invertebrate biodiversity. *Science* 367:272–277.
- Fink, W. L. 1982. The conceptual relationship between ontogeny and phylogeny. *Paleobiology* 8:254–264.
- Foth, C., B. P. Hedrick, and M. D. Ezcurra. 2016. Cranial ontogenetic variation in early saurischians and the role of heterochrony in the diversification of predatory dinosaurs. *PeerJ* 4:e1589.
- Gerber, S., P. Neige, and G. J. Eble. 2007. Combining ontogenetic and evolutionary scales of morphological disparity: a study of early Jurassic ammonites. *Evolution and Development* 9: 472–482.
- Godoy, P. L., G. S. Ferreira, F. C. Montefeltro, B. C. Vila Nova, R. J. Butler, and M. C. Langer. 2018. Evidence for heterochrony in the cranial evolution of fossil crocodyliforms. *Palaeontology* 61:543–558.
- Gould, S. J. 1977. *Ontogeny and phylogeny*. Belknap Press of Harvard University Press, Cambridge, Mass.
- Groves, J. R., and Y. Wang. 2009. Foraminiferal diversification during the late Paleozoic ice age. *Paleobiology* 35:367–392.
- Groves, J. R., M. Pike, and K. Westley. 2012. A test for the possibility of photosymbiosis in extinct fusuline Foraminifera: size and shape related to depth of habitat. *Palaios* 27:738–751.
- Haeckel, E. 1866. *Generelle morphologie der organismen. Allgemeine grundzüge der organischen formen-wissenschaft, mechanisch begründet durch die von Charles Darwin reformirte descendenztheorie*. Georg Reimer, Berlin.
- Haeckel, E. 1905. *The evolution of man*. Translated by J. McCabe. G. P. Putnam, New York.
- Hemleben, C., M. Spindler, and O. Erson. 1989. *Modern planktonic foraminifera*. Springer, Berlin.
- Hohenegger, J. 2011. Growth-invariant meristic characters tools to reveal phylogenetic relationships in Nummulitidae (Foraminifera). *Turkish Journal of Earth Sciences* 20:655–681.
- Hohenegger, J., and A. Briguglio. 2014. Methods for estimating individual growth of foraminifera based on chamber volumes. Pp. 29–54 in H. Kitazato, and J. M. Bernhard, eds. *Approaches to study living foraminifera*. Springer, Tokyo.
- James, E. 1823. *Account of an expedition from Pittsburgh to the Rocky Mountains, performed in the years 1819 and 1820*. H. C. Carey and I. Lea, Philadelphia.
- Jones, D. S. 1988. Sclerochronology and the size versus age problem. Pp. 93–108 in M. L. McKinney, ed. *Heterochrony in evolution: a multidisciplinary approach*. Springer, New York.

- Kahler, F., and G. Kahler. 1937. Beiträge zur Kenntnis der Fusuliniden der Ostalpen: Die Pseudoschwagerinen der Grenzlandbänke und des oberen Schwagerinenkalkes. *Palaeontographica* 87:1–44.
- Klingenberg, C. P. 1998. Heterochrony and allometry: the analysis of evolutionary change in ontogeny. *Biological Reviews* 73:79–123.
- Klingenberg, C. P., and J. R. Spence. 1993. Heterochrony and allometry—lessons from the water strider genus *Limnoporus*. *Evolution* 47:1834–1853.
- Lee, J. S. 1927. Fusulinidae of North China. *Paleontologica Sinica* series B 4:1–123.
- Leven, E. Y. 1993. Main events in Permian history of the Tethys and fusulinids. *Stratigraphy and Geological Correlation* 1:51–65.
- Likharev, B. K. 1934. On the question of the age of the Safet-Daron limestone in Darwas. Reports of the Academy of Sciences USSR 4:180–184. [In Russian.]
- Likharev, B. K. 1939. An atlas of the leading forms of the fossil fauna of the USSR, Vol. 6. Permian. Central Geological and Prospecting Institute, Leningrad. [In Russian.]
- Liu, C., X. Xiao, and W. Dong. 1978. Protozoa. Pp. 12–98 in Guizhou Stratigraphical and Paleontological Team, ed. *Paleontological atlas of Southeast Area, Guizhou Province (2), Carboniferous–Quaternary*. Geological Publishing House, Beijing. [In Chinese.]
- MacLeod, N. 1999. Generalizing and extending the eigenshape method of shape space visualization and analysis. *Paleobiology* 25:107–138.
- MacLeod, N. 2008. Size & shape coordinates. *Palaeontological Association Newsletter* 69:26–36.
- MacLeod, N. 2009. Shape theory. *Palaeontological Association Newsletter* 71:34–47.
- McKinney, M. L. 1988. Classifying heterochrony: allometry, size, and time. Pp. 17–34 in M. L. McKinney, ed. *Heterochrony in evolution: a multidisciplinary approach*. Springer, New York.
- McKinney, M. L., and K. J. McNamara. 1991. *Heterochrony: the evolution of ontogeny*. Springer, New York.
- McNamara, K. J. 1986. A guide to the nomenclature of heterochrony. *Journal of Paleontology* 60:4–13.
- McNamara, K. J., and J. A. Long. 2012. The role of heterochrony in dinosaur evolution. Pp. 761–784 in M. K. Brett-Surman, J. Thomas R. Holtz, J. O. Farlow, and B. Walters, eds. *The complete dinosaur*. Indiana University Press, Bloomington.
- Merchant, F. E., and R. P. Keroher. 1939. Some fusulinids from the Missouri Series of Kansas. *Journal of Paleontology* 13:594–614.
- Mitteroecker, P., P. Gunz, and F. L. Bookstein. 2005. Heterochrony and geometric morphometrics: a comparison of cranial growth in *Pan paniscus* versus *Pan troglodytes*. *Evolution and Development* 7:244–258.
- Murray, J. W. 2006. *Ecology and applications of benthic foraminifera*. Cambridge University Press, Cambridge.
- Neige, P., D. Marchand, and B. Laurin. 1997. Heterochronic differentiation of sexual dimorphs among Jurassic ammonite species. *Lethaia* 30:145–155.
- O’Keefe, F. R., O. Rieppel, and P. M. Sander. 1999. Shape disassociation and inferred heterochrony in a clade of pachypleurosaurs (Reptilia, Sauropterygia). *Paleobiology* 25:504–517.
- Oschmann, W. 2009. Sclerochronology: editorial. *International Journal of Earth Sciences* 98:1–2.
- Payne, J. L., J. R. Groves, A. B. Jost, T. Nguyen, S. E. Moffitt, T. M. Hill, and J. M. Skotheim. 2012. Late Paleozoic fusulinoid gigantism driven by atmospheric hyperoxia. *Evolution* 66:2929–2939.
- Raff, R. A. 1996. *The shape of life: genes, development, and the evolution of animal form*. The University of Chicago Press, Chicago.
- Rausser-Chernousova, D. M. 1938. The Upper Paleozoic foraminifera of Samara Bend and the Trans-Volga region. Proceedings of the Geological Institute of the USSR Academy of Sciences 7:69–168. [In Russian.]
- Rausser-Chernousova, D. M. 1958. High resolution subdivision of Upper Carboniferous section in the Kuibyshev Hydro-electric power station area. Proceedings of the Geological Institute of the USSR Academy of Sciences 13:121–138. [In Russian.]
- Rausser-Chernousova, D. M., and S. F. Shcherbovich. 1949. *Schwagerina* from the European part of the USSR. Reports of the Geological Institute Academy of Sciences USSR 105:61–117. [In Russian.]
- Rausser-Chernousova, D. M., G. Belyaev, and E. Reitlinger. 1936. Upper Paleozoic foraminifera of the Pechora region. Proceedings of the Polar Commission AS USSR 28:159–232. [In Russian with German abstract.]
- Roberts, T. J. 1949. Upper Paleozoic of Peru, Part 3: Fusulinidae. *Geological Society of America Memoir* 58:166–226.
- Rohlf, F. J., and D. Slice. 1990. Extensions of the Procrustes method for the optimal superimposition of landmarks. *Systematic Zoology* 39:40–59.
- Ross, C. A. 1967. Development of fusulinid (Foraminiferida) faunal realms. *Journal of Paleontology* 41:1341–1354.
- Ross, C. A. 1995. Permian fusulinaceans. Pp. 167–185 in P. A. Scholle, T. M. Peryt, and D. S. Ulmer-Scholle, eds. *The Permian of northern Pangea*. Springer, Berlin.
- Ross, C. A., and W. W. Tyrrell. 1965. Pennsylvanian and Permian Fusulinids from the Whetstone Mountains, Southeast Arizona. *Journal of Paleontology* 39:615–635.
- Rozovskaya, S. E. 1950. The genus *Triticites*, its development and stratigraphic significance. Proceedings of the Paleontological Institute 26:3–78. [In Russian.]
- Rozovskaya, S. E. 1975. Composition, phylogeny and system of the order Fusulinida. *Trudy Paleontologicheskogo Instituta Akademii Nauk SSSR* 149:1–267. [In Russian.]
- Schellwien, E. 1898. Die Fauna des Karnischen Fusulinenkalks. *Palaeontographica* 24:237–282.
- Schellwien, E. 1908. Monographie der Fusulinen. 1. Die Fusulinen des russisch-arktischen Meeresgebietes. *Palaeontographica* 55:145–194.
- Schwager, C. 1883. Die Foraminiferen aus den Eocaenablagerungen der libyschen Wüste und Aegyptens. *Palaeontographica* 30: 79–153.
- Shea, B. T. 1983. Allometry and heterochrony in the African apes. *American Journal of Physical Anthropology* 62:275–289.
- Sheng, J. C. 1949. On the occurrence of *Zellia* from the Maping limestone of Chengkung, Central Yunnan. *Bulletin of the Geological Society of China* 29:105–109.
- Sheng, J. Z., Y. J. Wang, and B. Z. Zhong. 1984. Some species of the genus *Robustoschwagerina* from Eastern Yunnan. *Acta Palaeontologica Sinica* 23:523–530. [In Chinese with English abstract.]
- Sheng, J. Z., L. X. Zhang, and J. H. Wang. 1988. Fusulinids. Science Press, Beijing. [In Chinese.]
- Shi, Y. K., and N. MacLeod. 2016. Identification of life-history stages in fusulinid foraminifera. *Marine Micropaleontology* 122:87–98.
- Shi, Y. K., and X. N. Yang. 2005. A statistical test on diversity changes of Early and Middle Permian fusulinacean fauna in South China. *Science in China Series D, Earth Sciences* 48:978–984.
- Shi, Y. K., J. R. Liu, X. N. Yang, and L. M. Zhu. 2009a. Fusulinid faunas from the Datangian to Chihhsian strata of the Zongdi Section in Ziyun county, Guizhou province. *Acta Micropalaeontologica Sinica* 26:1–30. [In Chinese with English abstract.]
- Shi, Y. K., X. N. Yang, and H. Huang. 2009b. Differences between subfamilies in diversification process of the Early and Middle Permian fusulinid fauna in South China. *Palaeoworld* 18:34–40.
- Shi, Y. K., X. N. Yang, and J. R. Liu. 2012. Early Carboniferous to Early Permian fusulinids from Zongdi Section in southern Guizhou. Science Press, Beijing. [In Chinese with English abstract.]

- Speijer, R. P., D. Van Loo, B. Masschaele, J. Vlassenbroeck, V. Cnudde, and P. Jacobs. 2008. Quantifying foraminiferal growth with high-resolution X-ray computed tomography: new opportunities in foraminiferal ontogeny, phylogeny, and paleoceanographic applications. *Geosphere* 4:760–763.
- Thompson, M. L. 1954. American Wolfcampian fusulinids. University of Kansas Paleontological Contributions, Article 5:1–226.
- Thompson, M. L., G. J. Verville, and H. J. Bissell. 1950. Pennsylvanian Fusulinids of the South-Central Wasatch Mountains, Utah. *Journal of Paleontology* 24:430–465.
- Webster, M., and M. L. Zelditch. 2005. Evolutionary modifications of ontogeny: heterochrony and beyond. *Paleobiology* 31:354–372.
- Wei, K. Y. 1994. Allometric heterochrony in the Pliocene–Pleistocene planktic foraminiferal clade *Globocornella*. *Paleobiology* 20:66–84.
- White, M. P. 1932. Some Texas Fusulinidae. *Texas University Bulletin* 3211:1–105.
- Xiao, W. M., H. D. Wang, and L. X. Zhang. 1986. Early Permian stratigraphy and faunas in southern Guizhou. People's Publishing House of Guizhou, Guiyang. [In Chinese with English abstract.]
- Yang, X. N., 1982. Fusulinids from the Maping formation of Guangxi. Master's thesis. Nanjing University, Nanjing. [In Chinese with English abstract.]
- Yang, X. N. 1992. A study of ontogeny and evolution of *Robustoschwagerinids* (Permian fusulinids). Pp. 127–133 in *Studies in Benthic Foraminifera, Benthos '90*. Tokai University Press, Sendai.
- Yang, X. N., and Y. C. Hao. 1991. A study on ontogeny and evolution of *Robustoschwagerinids* (Permian fusulinids). *Acta Palaeontologica Sinica* 30:277–306. [In Chinese with English abstract.]
- Yang, X. N., J. R. Liu, L. M. Zhu, and G. J. Shi. 2005. Early Permian bioevent in the fusulinacean fauna of South China. *Lethaia* 38:1–16.
- Zhang, L. X. 1963. Late Carboniferous Fusulinids of Keping and the adjacent area, Xinjiang (II). *Acta Palaeontologica Sinica* 11:200–239. [In Chinese with Russian abstract.]
- Zhang, L. X. 1982. Fusulinids of eastern Qinghai-Tibet Plateau. Pp. 119–244 in *Bureau of Geology of Sichuan Province and CAS Nanjing Institute of Geology and Palaeontology, eds. The stratigraphy and palaeontology of West Sichuan and East Tibet*. Sichuan People's Publishing House, Chengdu. [In Chinese with English abstract.]
- Zhang, L. X., L. Rui, J. M. Zhao, Z. R. Zhou, C. Y. Wang, Z. H. Wang, Z. H. Wang, C. Q. Li, H. Y. Li, P. Q. Kang, and D. Zhong. 1988. Permian fossil materials in Southern Guizhou. People's Publishing House of Guizhou, Guiyang. [In Chinese.]
- Zhang, L. X., J. P. Zhou, and J. Z. Sheng. 2010. Upper Carboniferous and Lower Permian fusulinids from western Guizhou. Science Press, Beijing. [In Chinese with English abstract.]
- Zhou, J. P., and X. N. Yang. 1996. *Zellia* (Fusulinid) from Guangxi and Guizhou. *Acta Palaeontologica Sinica* 35: 600–606. [In Chinese with English abstract.]
- Zollikofer, C. P. E., and M. S. P. De León. 2006. Cranial growth models: heterochrony, heterotopy, and the kinematics of ontogeny. Pp. 89–112 in K. Harvati and T. Harrison, eds. *Neanderthals revisited: new approaches and perspectives*. Springer, Dordrecht, Netherlands.